Numerical study on the tropospheric oxidants budget in East Asia and effects of intruding stratospheric ozone on it

Hiromasa Ueda[1)] & Suk-Jai Kang[2)]
1) Disaster Prevention Research Institute, Kyoto University, Uji, Kyoto 611-0011, Japan,
E-mail ueda@bouhuu.dpri.kyoto-u.ac.jp
2) Graduate School of Earth Sci. and Tech., Kyushu University, Kasuga, Fukuoka 816-0016, Japan
E-mail: kang@riam.kyushu-u.ac.jp

Abstract

Ozone intrusion from stratosphere into troposphere and its effects on the tropospheric oxidants budget in East Asia were investigated. Intense ozone intrusion was found to occur in southwest China and northwest Pacific rims near Japan and northeast China, which contributed to the highest ozone concentration in the world. While, in the lowest troposphere photochemical oxidant formation from anthropogenic pollutants was active and created regional-scale high-concentration ozone in the atmospheric boundary layer. Transboundary photochemical oxidants pollution in eastern China, Korea and Japan was caused by the long range transport of this regional-scale high concentration ozone.

1 Introduction

Atmospheric environment in East Asia is characterized by high concentrations of regional tropospheric ozone and dust. The tropospheric ozone concentration and dust fall in spring are at highest levels in the world and the high concentration area is also largest, extending from East

Asia to Northwest Pacific Ocean (Ueda and Carmichael [1]). Pollution level of precipitation, i.e., sulfate and nitrate concentration in rain and snow, in East Asia is also be-coming higher than Europe and North America.

In spite of these severe pollution conditions, emission of air pollutants is increasing rapidly. For example, total SOx emission in Asia in 1998 is almost the same level as that in Europe and supposed to become twice by 2010. Therefore, East Asia is now going to face atmospheric environmental problems that we have never experienced.

Regional tropospheric ozone issues were investigated in the present work. Tropospheric ozone is caused by active intrusion of stratospheric air mass into troposphere and by photochemical reactions of anthropogenic air pollutants during long range transport. At first, amount of stratospheric ozone intrusion averaged for four seasons was estimated from the vertical wind of ECMWF fine mesh data of 1993 and the ozone concentration of the worldwide ozonesonde observation network. Next, using the stratospheric ozone intrusion, together with anthropogenic emissions of NOx, SOx and volatile hydro-carbons, as the boundary conditions, tropospheric oxidants formation was simulated over the domain of 19-52 deg. N and 84-160 deg. E by means of a sophisticated numerical model of transport, chemistry and deposition of air pollutants (STEM II model, Carmichael et al. [2], Chang et al. [3, 4]). From the numerical results budget of tropospheric oxidants for each season was investigated for whole and sub-layers of the troposphere over Japan and other subdomains in East Asia.

2 Calculation of Ozone Intrusion

2.1 Analyzed domain

The domain analyzed was 19-52 deg. N and 84-160 deg. E, which covered China, Korea, Taiwan, Japan, parts of Russia and Mongolia and the North West Pacific Ocean. The total length of latitude was 4950km and that of longitude was 3450km. Horizontal grids was uniform with grid size of 75km and in the vertical direction, 17 variable grids were used up to 24km.

2.2 Ozone intrusion from stratosphere

For meteorological inputs, the analyzed fine-mesh ECMWF

data with longitudinal and latitudinal resolutions of 0.75 deg. and time resolution of 6 hours, for the analyzed domain and for the year of 1993, was used, which included wind flow, temperature, pressure, humidity and cloud cover index. It was de-fined at 15 vertical layers from the earth's surface to 10 hPa.

For ozone, data set of ozone profiles observed at four aerological observatories, Sapporo, Tsukuba, Kagoshima and Naha in Japan every one week and extended at latitudes from 43 to 26 deg. N, along with a few data in Taiwan (22 deg. N) and the other Asian countries were referred from Annual Report of Worldwide Ozone Observatories published by Japan Meteorological Agency and Akimoto et al.[5].

Seasonal averages of meteorological fields at 00:00, 06:00, 12:00 and18:00 GMT for grid cells over the analyzed domain was obtained from the data set of 1993. Interpolating the vertical profiles and tropopause heights in East Asia, seasonal mean ozone intrusion from stratosphere into troposphere was calculated from vertical velocity and ozone concentration at the tropo-pause.

3 Calculation of Tropospheric Ozone Formation and Transport

3.1 Numerical model for transport/diffusion/chemistry deposition of pollutants in troposphere

The numerical model for transport/ turbulent diffusion/ chemistry/ deposition used is an sophisticated Eulerian model (STEM II model, Carmichael et al. [2], Chang et al , [3, 4]). This model is a three-dimensional Eulerian model. The chemistry module is based on the chemical mechanism of Lurman et al. [6]) which treats 53 chemical species in the gas, cloud, rain and snow phases. Thirty six species are advected, while the remaining species are short-lived and are modeled using pseudo-steady state approximation. The numerical integration of the chemistry is based on a semi-implicit Euler method.

The model uses the surface-following coordinate system. Vertical eddy diffusivity was calculated for stable and neutral stratification conditions by Shir [7] and for unstable conditions by Lamb and Duran [8]. Horizontal eddy diffusivity was held constant. Dry deposition velocity was calculated as the reciprocal of sum of

aerodynamic resistance, surface resistance and residual resistance (Wesely et al. [9]). Land use was divided into 7 types i.e., sea, desert, agriculture area, grasslands, urban area, coniferous forest and broad-leaf forest. Cloud cover index was used to determine atmospheric stability (Pasquill [10]) for the calculation of deposition velocity and eddy diffusivity.

The ECMWF data for every 6 hours were interpolated temporally with 30 minutes interval for simulation and spatially for the present coordinate system. Vertical velocity was modified, using the divergence theorem in order to avoid mass balance inconsistencies.

3.2 Emission data and simulation procedure

In the calculation of tropospheric ozone formation and transport, ground surface emissions were used, together with the stratospheric ozone concentration, as input data for the numerical model of transport/ diffusion/ chemistry/ deposition. Emission source distribution by Akimoto and Narita [11] from fuel combustion and industrial activities with 1 deg. x 1 deg. was used for SOx and NOx emissions. Volatile hydrocarbon emissions were from Piccot et al. [12]. Seasonal variations in emission were considered by GEIA data [13] and emissions in daytime was assumed 1.5 times of daily-average, a half at night.

At the top boundary and inflow side boundary, ozone concentration was fixed at the observed seasonal average and concentrations of other species were those predicted for clean background area by one-dimensional version of the present model. At the outflow side boundary, zero gradients of the concentrations were applied. Initial conditions at ground surface in Japan and Korea were based on the atmospheric monitoring data and those in other region were estimated by values of similar area in Japan and Korea on reference to NOx and SOx emissions. Vertical profiles were also those predicted by the one-dimensional version.

Numerical integration was achieved by the fractional time steps and one dimensional finite element methods, referred to as the Locally One-dimensional Finite Element Method (LOD-FEM) (Yaneko [14]). The LOD procedure splits the multi-dimensional partial differential equations into time-dependent one-dimensional problems which are solved sequentially. Here, the chemical reaction term was treated separately because of the fact that many chemical reactions had much

shorter characteristic time scales than those of transport. Thus, different time steps were applied for transport (900sec) and chemical reaction (60sec).

4 Results and Discussion

4.1 Seasonal averaged wind fields and comparison of predicted ozone profiles with observations

Figure 1 shows the seasonal averaged wind fields and trajectories at 1.5 km level. With increasing height the zonal westerly winds prevailed at mid-latitudes, i.e., in the northern half of the domain where the seasonal winds from Siberia were superimposed on them and westerly winds prevailed even at the ground level in winter and spring. In contrast, in the southern half of the domain, i.e., subtropical region, wind fields were complicated by Asian monsoon and zonal easterly winds in summer hemisphere. The Asian monsoon was intensified typically in the Southeast Asia and southerly winds covered in the Pacific rim region even at higher latitudes.

Predicted ozone profiles at 4 observatories in Japan were compared with observed ones. As an example, springtime profiles were presented in Fig.2. Agreement was fairly well. It was also in case for other seasons. It indicates the validity of the present estimation of tropospheric ozone formation with the ozone intrusion at the top boundary.

4.2 Regional ozone field

Outlook of the regional ozone field in East Asia (not shown) was as follows.

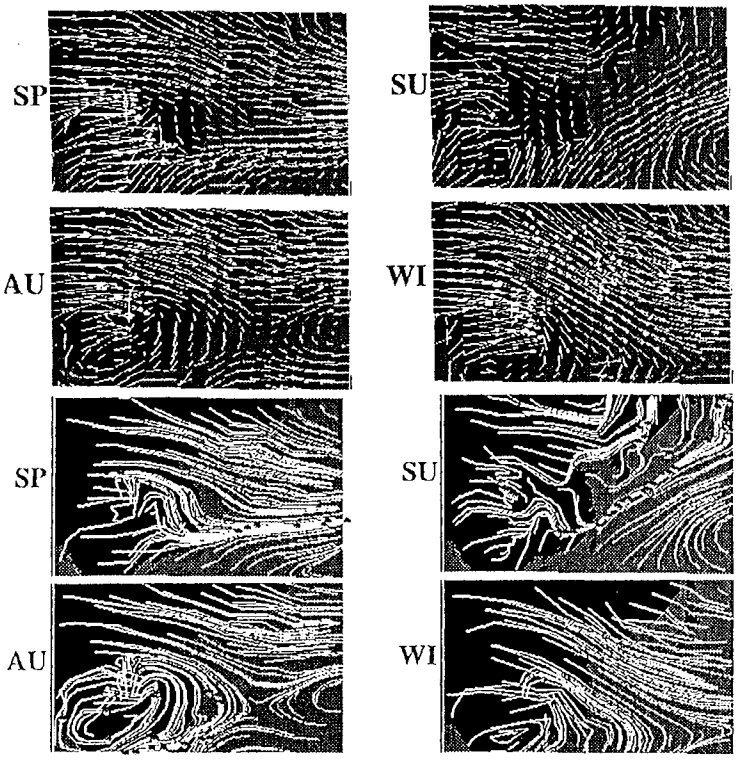

Fig.1 Seasonal averaged wind fields and trajectories at 1.5 km level in spring (SP), summer (SU), autumn (AU) and winter (I).

For all seasons, the ozone concentration in the layer from the earth's surface to 0.7 km was relatively high. It was decreased with increasing height and remained at low level in the layer from 3 km to 9 km and then increased again from 10km level to the maximum at the top boundary of the model in stratosphere. Relatively high concentration in the lowest layer was attributed to the active photochemical formation from ground surface emissions.

In spring, high concentration ozone with the maximum of 100ppb was distributed uniformly over the Asian continent at 0.7 km level. The ozone distribution at this height was similar in summer although the concentration level was lower. However, in autumn and winter high concentration zone was limited to north and southeast China with almost the same concentration level as that in spring.

In the layer from 3km to 9km ozone concentration was lowest in general but a significantly high concentration zone was formed in

southeast China at 6 km and upper levels. This concentration attained 130ppb in spring and 100ppb, 75ppb and 100ppb in summer, autumn and winter, respectively. This high concentration zone extended in space and its concentration increased, with increasing height, and finally at 14 km level the concentration reached at 300ppb, 330ppb, 300ppb and 240ppb in spring, summer, autumn and winter.

Formation of the high concentration zone was supposed to be attributed to the interaction between zonal westerly winds and Himalayas and Tibet plateau.

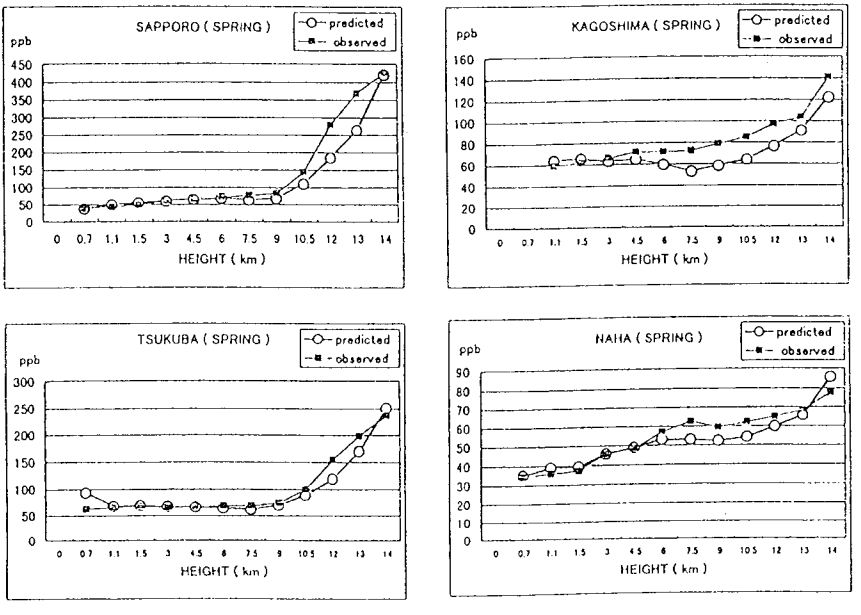

Fig.2 Comparison between predicted and observed ozone profiles in spring.

Chen [15] and Dunkerton [16] emphasized the role of summer monsoon circulation in stratosphere-troposphere (S/T) exchange. Chen [15] found that isentropic mixing and S/T exchange in the "upper middle world" were significant in northern summer, in connection with Asian and Mexican monsoons. The S/T exchange in Asian monsoon was much more vigorous than that in Mexican monsoon. This vigorous S/T exchange .was observed mainly due to wave transience and the irreversible mixing and transport by breaking synoptic-scale disturbances. In fact, quasi-stationary Rossby waves usually broke in the periphery of

Himalayas and Tibet plateau in middle and higher latitudes. For the same reason another high concentration zone appeared at 10.5 km level in northeastern China.

At 10.5km level higher ozone concentration was observed in the northern part of the analyzed domain, reflecting to the lower tropopause height at higher latitudes. Remarkably high concentration zone appeared also in the northern Pacific rim region. This high concentration zone was considered to be attributed to the tropopause folding caused by active moving high-pressure system and by lower tropopause height (Wakamatsu et al. [17]).

4.3 Ozone intrusion from stratosphere and ozone budget

Figure 3 shows the seasonal distribution of vertical wind in the upper troposphere and lower stratosphere. Significantly large downward motion was seen in the southern Asian continent even at 15 km level in summer. It was more than 5 times larger than that over the southern Pacific ocean. In the northern part of the domain the vertical motion was very weak.. In contrast, in

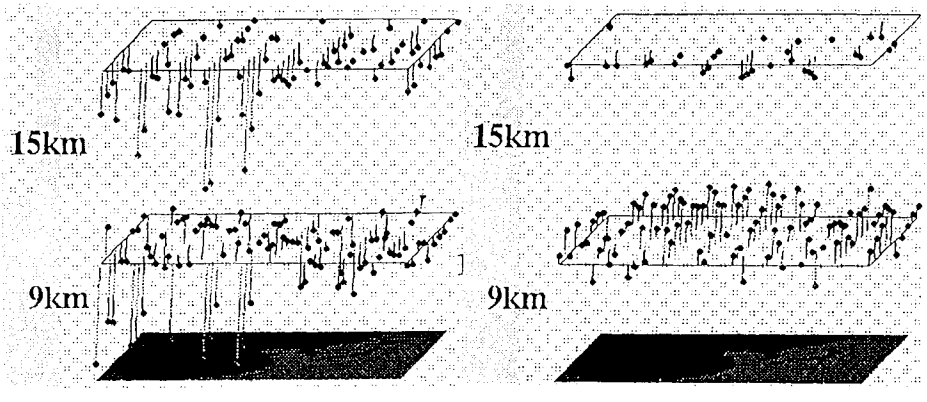

(a) Summer (b) Winter

Fig.3 Distributions of vertical velocity over East Asia in summer and winter.

winter weak upward motions prevailed in the upper troposphere (not shown).Tropopause height was low and the 15 km level was considered to be in stratosphere.

Ozone budget was investigated from the vertically-integrated form of ozone conservation equation which consisted of accumulation, horizontal advection, vertical advection, turbulent diffusion, chemical formation and deposition terms. Ozone intrusion at tropopause from stratosphere was caused mainly by downward advection and slightly by turbulent diffusion. In order to make clear the regional characteristics, the analyzed domain was divided horizontally into 8 sub-domains, i.e., west China, east China, south Korea, north Korea, north Japan, central Japan, south Japan and Taiwan, and vertically into 6 layers up to stratosphere. Flux of ozone intrusion was presented in Fig. 4, together with chemical formation and horizontal advection. In spite that southeast China with strongest downward motion in the upper troposphere was categorized into west China, ozone intrusion flux in west China was largest among the subdomains. Remarkably large flux in summer resulted in a large yearly average. In spring, however, intrusion flux in east China, Korea and Japan was larger, which was considered to be due to the tropopause folding caused by active moving high pressure systems, while in autumn and winter upward ozone flux into stratosphere which was attributed to the weak upward motion at tropopause were observed there.

Tropospheric ozone formation by reactions was reflected by the difference in emission strength. That was, strong emission sources in Japan and south Korea contributed ozone formation, while ozone depression was remarkable in China when averaged throughout the troposphere column.

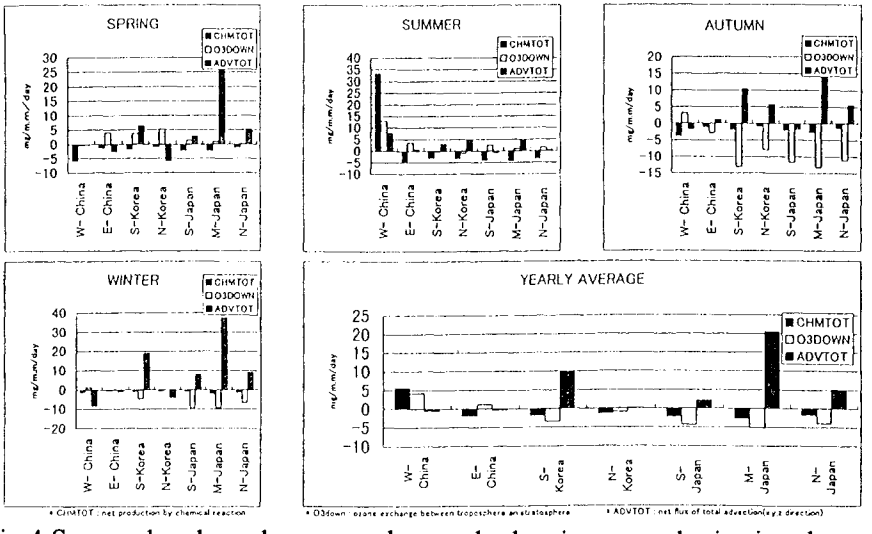

Fig.4 Seasonal and yearly averaged ozone budget in tropospheric air columns.

4 Conclusion

Intense ozone intrusion from stratosphere into troposphere was found to occur in southwest and northwest China downstream the high mountainous areas, i.e., Himalayas and Tibet plateau. Active intrusion of stratospheric ozone was also seen in northwest Pacific rims near Japan and northeast China. The former was suspected to be caused by interaction between zonal westerly winds and high and massive mountains and the latter was attributed to tropo-pause folding caused by active moving high pressure systems. These mechanisms was considered to contribute to the highest ozone level in the world.

Amount of these intrusion was in the same order of magnitude as chemistry formation in troposphere and horizontal advection and it contributed active photochemical oxidants formation in the upper troposphere of more than 9km high. Chemical reactions worked to destruct ozone and so decreased the ozone concentration in the middle and lower troposphere with decreasing height, although the concentration level being still strongly affected by the stratospheric ozone intrusion. This vertical profile was seen in subdomains far from large emission

sources, typically in China and over the ocean. However, in the lowest troposphere over emission source areas and surroundings photochemical oxidant formation from anthropogenic pollutants was active and created regional-scale high-concentration ozone in the atmospheric boundary layer in which ozone concentration level was sometimes more than 100-150 ppb. Transboundary photochemical oxidants pollution in eastern China, Korea and Japan was caused by the long range transport of this regional-scale high concentration ozone which was limited in the layer of 0-3km high.

References

[1] Ueda, H. and Carmichael, G.R., Formation of secondary pollutants during long-range transport and its contribution to air quality in East Asia, *Terres., Atmos. Oceanic Sci.*, **6**, pp.487-500, 1995.

[2] Carmichael, G.R., Peters, L.K. and Kitada, T., A second generation model for regional-scale transport/chemistry/deposition. *Atmos. Environment*, **20**, pp.173 -188, 1986.

[3] Chang, Y.S., Carmichael, G.R., Kurita, H. and Ueda, H., The transport and formation of sulfates and nitrates in central Japan. *Atmos. Environment*, **23**, pp.1749-1773, 1989.

[4] Chang, Y.S., Shin, W.C., Carmichael, G.R., Kurita, H. and Ueda, H., Evaluation of the effect of emission reductions on pollutant levels in central Japan. *Environ. Sci. Technol.*, **24**, pp.1355-1366, 1990.

[5] Akimoto, H., Mukai, H., Nishikawa, M., Murano, K., Hatakeyama, S., Liu, C.M., Buhr, M., Hsu, K.J., Jaffe, D.A., Zhang, L., John, R.H., Merrill, T. and Newell, R.E., Long-range transport of ozone in the East Asian Pacific rim region, *J. Geophys. Res.*, **101**, pp.1999-2010, 1996.

[6] Lurman, F.W., Lloyd, A.C. and Atkinson, R., A chemical mechanism for use in long range transport/acid deposition computer modelling. *J. Geophys. Res.*, **91**, pp.10905-10936 (1986).

[7] Shir, C.C., A preliminary numerical study of atmospheric turbulent flows in the idealized planetary boundary layer. *J. Atmos. Sci.*, **30**, pp.1327-1339, 1973.

[8] Lamb, R.G., and Duran, D.R., Eddy diffusivities derived from a numerical model of the convective boundary layer. *Nov. Cement*, **1C**, pp.1-17, 1977.

[9] Wesely, M.L., Cook, D.R., Hart, R.L. and Speer, R.E., Measurements and parameterization of particulate sulfur dry deposition over grass. *J. Geophys. Res.*, **90**, pp.2131-2143, 1985.

[10] Pasquill, F., The estimation of the dispersion of windborne material. *Meteorol. Magazine*, **90**, pp.33-49, 1961.
[11] Akimoto, H. and Narita, H., Distribution of SO2, NOx and CO2 emission from fuel combustion and industrial activities in Asia with 1deg.x1 deg. resolution. *Atmos. Environment*, **28**, pp.213-225, 1994.
[12] Piccot, S., Watson, S.D. and Jones, J.W., A global inventory of volatile organic compound emissions from anthropogenic sources. *J. Geophys. Res.*, **97**, pp.9897-9912, 1992.
[13] GEIA, GEIA Data Management and Communication Center, 1997.
[14] Yonenko, N.N., The method of fractional pitches in solving many-dimensional problems of mathematical physics, NAUKA, Novosibirsk, 1967.
[15] Chen, P., Isentropic cross-tropopause mass exchange in the extratropics. *J. Geophys. Res.*, **100**, pp.16661-16673, 1995.
[16] Dunkerton, T.J., Evidence of meridional motion in the summer lower strato-sphere adjacent to monsoon regions. *J. Geophys. Res.*, **100**, pp. 16675-16688, 1995.
[17] Wakamatsu, S., Uno, I., Ueda, H., Uehara, K. and Tateishi, H., Observational study of stratospheric ozone intrusions into the lower troposphere, *Atmos. Environment*, **23**, pp.1815-1826, 1989.